Dynamics of CO elimination from reactions of yttrium atoms with formaldehyde, acetaldehyde, and acetone

Jonathan J. Schroden, Maurice Teo, and H. Floyd Davis[a)]
Department of Chemistry and Chemical Biology, Cornell University, Ithaca, New York 14853

(Received 24 June 2002; accepted 26 August 2002)

Reactions of neutral, ground-state yttrium atoms with formaldehyde, acetaldehyde, and acetone ($Y+RR'CO$, where $R,R'=H,CH_3$) were studied in crossed molecular beams. At collision energies greater than 24 kcal/mol, four product channels were observed corresponding to elimination of CO, H_2, H, and nonreactive scattering. For the dominant CO elimination channel, a large fraction (34%–41%) of the available energy appeared as kinetic energy of the products. RRKM modeling indicated this was a result of two factors: a large potential energy barrier for R' migration leading to $(R)(R')YCO$ and dissociation of this complex prior to complete energy randomization. The CM angular distributions were all forward–backward symmetric, indicating the existence of at least one long-lived reaction intermediate. The angular distributions ranged from being quite forward–backward peaking for the $Y+H_2CO$ reaction to isotropic for $Y+(CH_3)_2CO$. A simple equation is derived based on statistical complex theory that relates the shape of the CM angular distributions to the structure of the dissociating complex. © *2002 American Institute of Physics.*
[DOI: 10.1063/1.1514584]

I. INTRODUCTION

Migratory insertion reactions into metal–carbon bonds have been of interest for many years.[1,2] These reactions are important industrially and present challenging opportunities for mechanistic studies. Examples include insertion of unsaturated hydrocarbons such as ethylene and acetylene, as well as carbon monoxide.[2] A complete understanding of conditions affecting the rate and selectivity of these reactions is desirable, and much work has been done with this goal in mind.[1,2]

There have been a number of studies of intramolecular migratory insertion of a ligand *R* into a metal–carbon (M–C) bond in solution.[1] This work has addressed many questions including the role of spectator ligands, how the choice of metal center affects reactivity, and how insertion affects stereochemistry. A fundamental understanding of these reactions is of importance to the design of better catalysts. Important mechanistic questions have been addressed, such as whether reaction occurs via ligand insertion into the M-alkyl bond, or whether reaction instead involves migration of the alkyl group.[1] These two processes are illustrated in Fig. 1.

Useful mechanistic information can be obtained by studying the reverse of the reaction in Fig. 1, i.e., the process whereby a bare or partially-ligated metal atom inserts into the C–H or C–C bond (C–*R*) of a carbonyl-containing molecule. Some of the earliest such studies were those of Freiser *et al.*, who used ion–cyclotron resonance (ICR) spectroscopy to study reactions of Cu^+ and Fe^+ with acetaldehyde and acetone, among many others.[3,4] They found Cu^+ to be quite unreactive, while Fe^+ eliminated C_2H_6 and CO from acetone. These studies were repeated for Fe^+ and extended to include Co^+ and Ni^+ by Beauchamp and co-workers.[5] They also observed both C_2H_6 and CO elimination in reactions with acetone. However, reactions with acetaldehyde and formaldehyde yielded only CH_4 and H_2 elimination, respectively.[5] It was proposed that the product from CO elimination from acetone was $M(CH_3)_2^+$ rather than $M(C_2H_6)^+$.[4,5] Subsequently, Bowers and co-workers modeled the kinetic energy release distribution (KERDs) from reactions of Fe^+, Co^+, and Ni^+ with acetone and showed that formation of the ethane complex was dominant.[6] Statistical modeling of KERDs led to the conclusion that the rate limiting step for both CO and ethane elimination was insertion into the C–C bond of acetone.[6] This conclusion has been confirmed in recent crossed-beams studies.[7]

We have previously studied reactions of neutral gas-phase yttrium atoms with formaldehyde.[8] Both CO and H_2 elimination were observed at all collision energies studied (forming YH_2 and YCO, respectively). Due to the larger exothermicity of YH_2 formation and the existence of an exit channel barrier for elimination of H_2, the yield of YH_2+CO was much larger than that for $YCO+H_2$. A third reactive channel, formation of YCHO+H, was observed at a collision energy (E_{coll}) of 31 kcal/mol, but not at 16 kcal/mol.[8]

The reaction of yttrium with formaldehyde proceeds via C–H bond insertion, like many other reactions studied previously.[9–11] Recently, C–C bond activation in small molecules has been studied.[12] Formation of MCH_2, with elimination of ethylene, has been observed in reactions of ground-state Y, Zr, Nb, and excited-state Mo with cyclopropane.[12] This is perhaps not surprising, given the ring strain and theoretical predictions that the C–C insertion barrier should be lower than the C–H insertion barrier for Y and Mo.[13] Surprisingly, C–C bond activation was also observed in reac-

a)Author to whom correspondence should be addressed. Electronic mail: hfd1@cornell.edu

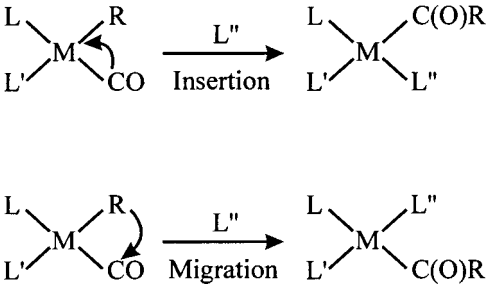

FIG. 1. Schematic reactions showing two mechanisms for insertion of CO into a metal–ligand (M–R) bond. (Top) Migratory insertion. (Bottom) Ligand migration. Adapted from Ref. 1.

tions of yttrium with propene, isobutene, *trans*-2-butene, propyne, and 2-butyne,[12] all hydrocarbons without ring strain.

Given the interest in reactions involving activation of C–C bonds, we extended our studies to the methylated analogs of formaldehyde, namely acetaldehyde and acetone. In all three reactions, several product channels are observed, including CO elimination, which involves cleavage of one C–C bond in the case of acetaldehyde, and remarkably, two C–C bonds in the case of acetone. The purpose of this report is to describe CO elimination from reactions of ground-state yttrium atoms with formaldehyde, acetaldehyde, and acetone. The other minor product channels will be described in detail in a separate publication that will include *ab initio* calculations.

II. EXPERIMENT

Experiments were carried out using a rotatable source crossed molecular beams apparatus.[14] The atomic yttrium beam was generated by focusing the 532 nm output of a Nd:YAG laser (Continuum Surelite) onto a 0.25-in. diam. yttrium rod (Alfa Aesar, 99.9%) that was rotated and translated by a screw assembly.[14] The ablated metal atoms were entrained in an inert gas[15] delivered by a piezoelectric pulsed valve.[16] The yttrium beam was collimated using a skimmer and crossed at 90° by a skimmed molecular beam. The molecular beam was produced using a second pulsed valve by passing 5 psig of inert carrier gas through a bubbler containing the molecular reactant, either solid paraformaldehyde (Aldrich, 95%), liquid acetaldehyde-d_4 (Aldrich, 99%),[17] or liquid acetone (Mallinckrodt, analytical grade). The bubbler containing the molecular reactant was held at a fixed temperature using either a silicon oil or methanol bath (98 °C for paraformaldehyde, −28 °C for acetaldehyde-d_4, 5 °C for acetone). The velocity distributions of both beams were measured by modulating the beams using a slotted chopper wheel and monitoring their time-of-flight (TOF) to the detector using electron impact ionization.[14] The yttrium beam has been characterized previously, and consisted only of ground state Y ($a\ ^2D_{1/2}$ and $a\ ^2D_{3/2}$) atoms.[9]

The metal-containing products drifted 24.1 cm to a detector, where they were ionized by the 157 nm output of an F_2 excimer laser (LPX220i).[14] Product TOF spectra were obtained by scanning the delay of the excimer laser trigger pulse with respect to a time zero for reaction, defined by the chopper wheel. By rotating the two beams with respect to the fixed detector, product TOF spectra were obtained. Integration of these spectra yielded the laboratory (lab) angular distribution, $N(\Theta)$. The TOF spectra and lab angular distribution were simultaneously fit using a forward-convolution program,[10] which required input of instrumental and experimental parameters (aperture sizes, flight distances, beam velocities, etc.), as well as the center-of-mass (CM) translational energy release distribution, $P(E)$, and CM angular distribution, $T(\theta)$. These two input functions were iteratively adjusted until optimal agreement was reached between simulated and experimental data.

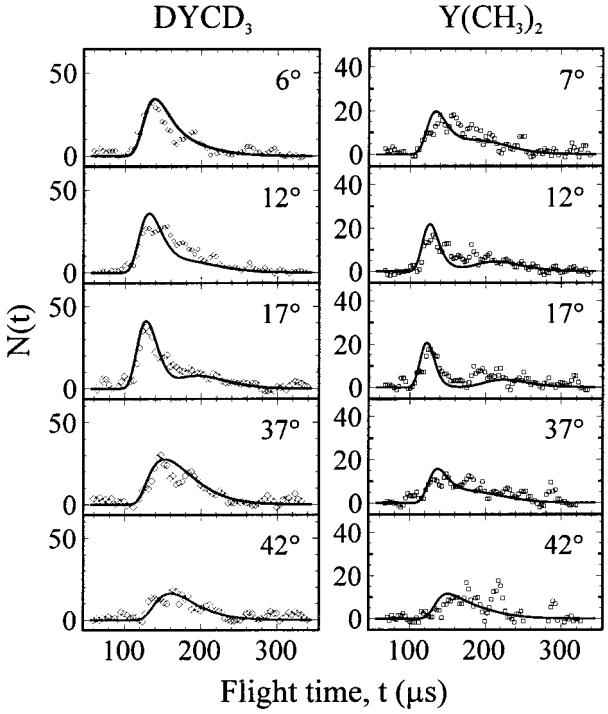

FIG. 2. Representative time-of-flight (TOF) spectra for CO elimination products in the reaction of $Y+CD_3CDO$ (left) and $Y+(CH_3)_2CO$ (right). Each TOF is the sum of 27 scans. Solid line fits generated using the center-of-mass (CM) distributions shown in Fig. 4.

III. RESULTS

In collisions of ground state Y ($a\ ^2D$) atoms with formaldehyde (H_2CO) at a collision energy (E_{coll}) of 27.0 kcal/mol, four processes were observed (detected products are underlined):

$$Y(a\ ^2D)+H_2CO \rightarrow \underline{YCHO}+H \quad \text{(i)}$$

$$\rightarrow \underline{YCO}+H_2 \quad \text{(ii)}$$

$$\rightarrow \underline{YH_2}+CO \quad \text{(iii)}$$

$$\rightarrow \underline{Y}+H_2CO. \quad \text{(iv)}$$

Process (iv) is nonreactive scattering. Analogous processes were observed in collisions of yttrium atoms with acetaldehyde and acetone. At this collision energy, CO elimination was the dominant process for all three reactions, with prod-

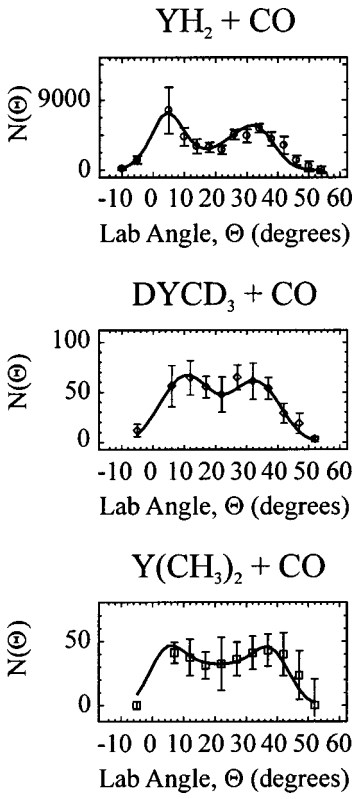

FIG. 3. Measured laboratory angular distributions for CO elimination products in the reactions (from top) $Y+H_2CO$, $Y+CD_3CDO$, and $Y+(CH_3)_2CO$ (open points). Solid line fits were generated using the CM distributions shown in Fig. 4.

uct fractions greater than 50% for acetaldehyde-d_4 and greater than 95% for formaldehyde and acetone.

The TOF spectra for the CO elimination channel for reactions of yttrium with acetaldehyde-d_4 and acetone are shown in Fig. 2. The TOF spectra for the analogous channel for the $Y+H_2CO$ reaction were presented previously.[8] Figure 3 shows the corresponding lab angular distributions. Due to the large exothermicity for elimination of CO (Refs. 13, 18, and 19) (see Table I) and the large mass of the recoiling CO counterfragment, the lab angular distributions span a wide range of angles.

The CM distributions used to generate the solid-line fits to the TOF spectra and lab angular distributions are shown in Fig. 4. The translational energy release distributions, $P(E)$, are quite similar for all three reactions, peaking away from zero kinetic energy and extending to nearly the thermodynamic limit (E_T). The average energy released into translation of products, $\langle P(E)\rangle$, is nearly identical for YH_2+CO and $DYCD_3+CO$, while that for CH_3YCH_3+CO is slightly greater, in part due to the larger amount of total energy available (E_T). In contrast to the $P(E)$s, the CM angular distributions are quite different in shape. The $T(\theta)$ for CO elimination from formaldehyde is quite similar to that reported previously at a collision energy of 20.9 kcal/mol.[8] It is sharply peaked in both the forward and backward directions ($\theta=0°$ and $\theta=180°$, respectively). The $T(\theta)$ for acetaldehyde is peaking to a much lesser extent than for formaldehyde, while the $T(\theta)$ for acetone is isotropic, with $T(\theta=0°)/T(\theta=90°)=1$ (Table II). The difference in the shape of the CM angular distributions can be more clearly seen in Fig. 5, where the CM product flux contour diagrams for the CO elimination products, generated by calculating $P(E)\times T(\theta)$, are shown. The change in the degree of forward–backward peaking is quite striking.

IV. DISCUSSION

A. Mechanism and structures

In our earlier report on the reaction of Y with H_2CO,[8] the energies of important stationary points along the reaction coordinate were estimated by comparison to calculations on yttrium+hydrocarbons. Subsequently, Bayse has performed *ab initio* calculations at the CCSD(T) level for the $Y+H_2CO$ and $Y+CH_3CHO$ systems[20] (Fig. 6). The reaction $Y+RR'CO$ (where R, $R'=H$, or CH_3) proceeds by formation of a donor–acceptor pi-complex involving the C═O bond. Yttrium can subsequently insert into either the $R-C$ or $R'-C$ bond, followed by migration of R and R' to the metal to form $(R)(R')Y(CO)$, which then decays to $RYR'+CO$. It should be noted that the product energetics in Fig. 6 and Table I (i.e., that of the $RYR'+CO$ asymptote) are based on experimental values.[13,18,19,21]

For formaldehyde, following pi-complex formation, insertion must be into a C–H bond. Similarly, in the reaction with acetone, the insertion is most likely into a C–C bond, followed by methyl migration. However, for acetaldehyde, reaction may proceed either by insertion into the C–H bond adjacent to the carbonyl followed by methyl migration, or by insertion into the C–C bond followed by H-atom migration. The strength of both bonds are quite similar: 87.9 ± 0.3 kcal/mol for the C–H bond adjacent to the carbonyl and 82.3 ± 0.3 kcal/mol for the C–C bond.[19] Bayse has found that both $(CH_3)YCHO$ and $(H)YCCH_3O$ lie about 40 kcal/mol below reactants. However, insertion into the C–H bond adjacent to the carbonyl encounters a potential energy barrier 8 kcal/mol smaller than that for C–C insertion.[20] This is not

TABLE I. Experimental conditions for $Y+RR'CO$ reactions.

Reactants	$\langle E_{coll}\rangle$[a]	v_Y[b]	$v_{RR'CO}$[b]	v_{rel}[b]	Θ_{CM}	μ[c]	μ'[c]	L_{max}	L'_{max}
$Y+H_2CO$	27.0	2369	2227	3252	18°	22.4	21.4	409$\hbar$	468$\hbar$
$Y+CD_3CDO$	24.6	2240	1550	2719	20°	31.2	22.3	499$\hbar$	503$\hbar$
$Y+(CH_3)_2CO$	32.0	2363	1402	2748	21°	35.1	22.7	610$\hbar$	551$\hbar$

[a]$\langle E_{coll}\rangle$ in kcal/mol.
[b]Velocities in m/s.
[c]Reduced masses in amu.

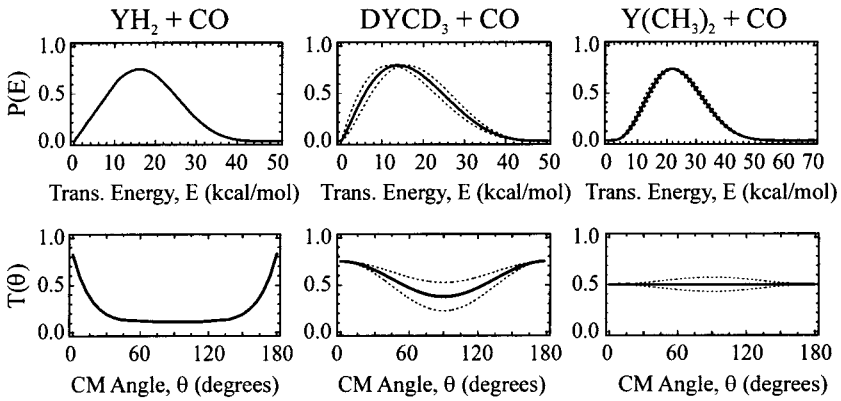

FIG. 4. CO elimination product center-of-mass (CM) distributions, $P(E)$s and $T(\theta)$s, for the reactions (from left) $Y+H_2CO$, $Y+CD_3CDO$, and $Y+(CH_3)_2CO$. Solid curves are the distributions that best fit the experimental data, whereas dashed curves represent the range of distributions that give acceptable fits to the data.

surprising given the spherical nature of the H 1*s* orbital and its ability to participate in multicentered bonding as opposed to the directional C–C bond.[22] One would expect a similar trend for potential energy barrier heights for the migration step, because the spherical 1*s* orbital of the H atom should migrate to the metal center more easily than the methyl group. Therefore, it is likely that CO elimination from Y+acetaldehyde could proceed through both mechanisms.

Structures for the complexes formed just prior to elimination of CO in the $Y+RR'CO$ reactions are depicted in Fig. 7. The structures of (H)(H)YCO and $(H)(CH_3)YCO$ shown are those calculated by Bayse.[20] For this discussion, $(D)(CD_3)YCO$ was assumed to have the same geometry as $(H)(CH_3)YCO$, and the structure of $(CH_3)(CH_3)YCO$ was estimated by assuming both Y–C bonds to be identical to that in $(H)(CH_3)YCO$. As in the gas-phase ion experiments, there is the question as to whether the product of these CO elimination reactions is actually RYR' or $Y(R-R')$. For neutral metal atoms, binding to hydrogen, methane, or ethane would be very weak (comparable to dispersion forces), so the products from these reactions must be RYR'.

B. Shape of the CM distributions

1. Translational energy distributions

The $P(E)$s for CO elimination (Fig. 4) peak quite far from the zero of kinetic energy, with 30%–40% of the available energy (E_T) appearing as translational energy (Table II). Figure 8 shows this more clearly, by plotting $P(f_T')$ versus f_T', the translational energy divided by E_T. In principle, this behavior might be due to the existence of a potential energy barrier for CO elimination from the final intermediate, $(R)(R)YCO$. However, this possibility may be ruled out by the calculations which found that CO elimination from (H)(H)YCO proceeds without a barrier in excess of the reaction endoergicity.[20] The potential energy surface for CO elimination in the acetaldehyde and acetone reactions should be similar.

For this class of reaction, the largest potential energy barrier along the reaction coordinate is that for R' migration forming $(R)(R')YCO$ (Fig. 6). This barrier lies 20 kcal/mol above the product asymptote, and inclusion of centrifugal effects will raise the effective height of this barrier even further. To investigate the role of centrifugal effects, RRKM calculations[23] were carried out for $Y+H_2CO$ using vibrational frequencies and moments of inertia calculated by Bayse.[20] The C–H insertion and H-atom migration barriers were treated as tight transition states, while dissociation of the pi-complex back to reactants and dissociation of (H)(H)YCO to YH_2+CO were treated as loose transition states. Variational calculations for the loose transition states were performed using simple C_6 potentials determined using polarizabilities of separated fragments.[24,25] Two of the degrees of freedom of the pi-complex were treated as internal rotations, corresponding to rotation of formaldehyde about the C–O axis and torsional rotation about the dissociating bond axis. The other degrees of freedom for this complex were treated as harmonic vibrations.

The ratio of the rate constant for rearrangement of the pi-complex to the final (H)(H)YCO complex $[k_{(H)(H)YCO}]$ to that for dissociation of the pi-complex back to reactants (k_{diss}) is shown in Fig. 9 as a function of total angular momentum $\mathscr{J}$ for several collision energies. We calculated $k_{(H)(H)YCO}$ by invoking the steady-state approximation for the complex formed after C–H activation (i.e., the second potential energy well as one reads from reactants to products in Fig. 6). At a collision energy of 27.0 kcal/mol, the cutoff is $\mathscr{J}=230\hbar$. Even at a very low collision energy of 5.0 kcal/mol, the cutoff is $\mathscr{J}=160\hbar$. Thus, even complexes with fairly large angular momentum, resulting from collisions

TABLE II. Energetics and CM distribution parameters.

Products	$\langle E_{coll}\rangle^a$	$\Delta E_{rxn}{}^a$	$E_T{}^a$	$\langle P(E)\rangle^a$	$E'_{pk}{}^a$	$\langle f_T'\rangle$	$T(\theta=0)/T(\theta=90)$	X
YH_2+CO	27.0	−22.3	49.3	17.3	16	0.352	7.49	8±1
$DYCD_3+CO$	24.6	−25.4	50.0	17.2	14	0.343	2.01	2.8±0.5
$Y(CH_3)_2+CO$	32.0	−26.4	58.4	23.7	22	0.406	1.00	0

[a]Energies in kcal/mol.

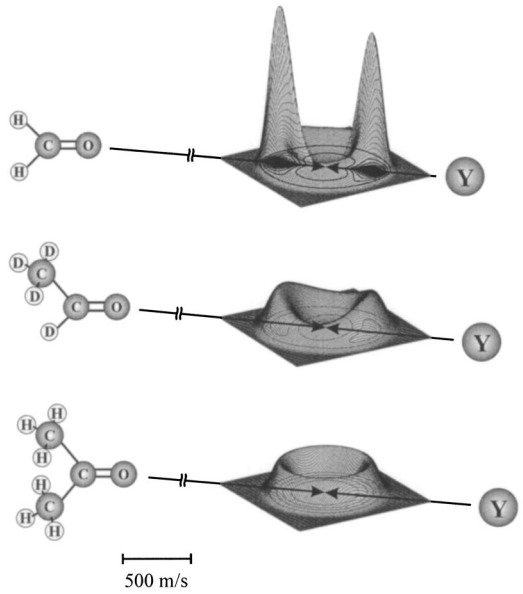

FIG. 5. Contour diagrams in the CM reference frame showing the distribution of CO elimination products from the reactions of (from top) $Y+H_2CO$, $Y+CD_3CDO$, and $Y+(CH_3)_2CO$. Diagrams are shown in velocity space.

with impact parameters as large as 3 Å, can surmount the large potential energy barrier and form (H)(H)YCO.

After the barrier leading to $(R)(R')$YCO is crossed, if excess energy cannot be channeled efficiently into vibrational and rotational energy as the complex dissociates to $RYR'+CO$, there will be a nonstatistical partitioning of the available energy into the products, yielding a $P(E)$ that will peak significantly away from the zero of energy.[26] Several important factors likely contribute to inefficient energy randomization prior to CO elimination. Using RRKM theory for the $Y+H_2CO$ reaction, the rate constant for dissociation of (H)(H)YCO to YH_2 and CO was $\approx 10^{14}$ s^{-1}, which is greater than even the largest vibrational frequency in the complex. Since energy will clearly not be fully randomized in the complex, the calculated RRKM rate is actually a lower

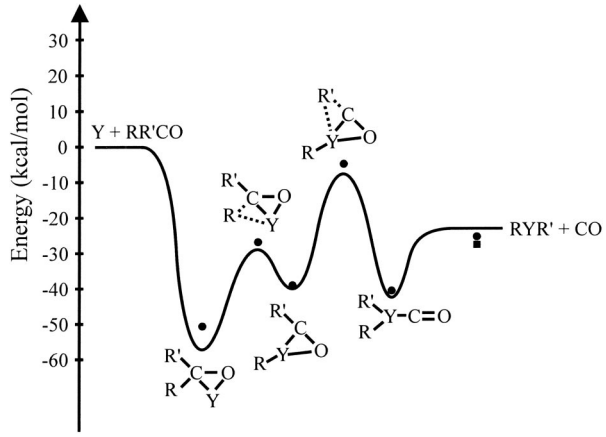

FIG. 6. Potential energy diagrams for the reactions of $Y+RR'CO(R,R'=H,CH_3)$. Solid lines show stationary points for $Y+H_2CO$, circles for $Y+CH_3CHO$, and squares for $Y+(CH_3)_2CO$. All values taken from Ref. 20 except $RYR'+CO$ asymptotes which are calculated using Refs. 13, 18, and 19.

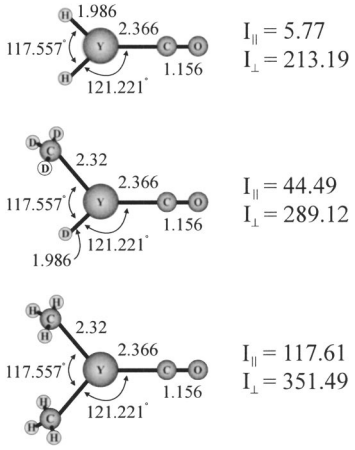

FIG. 7. Structures and moments of inertia (in amu/Å^2) of the dissociating $(R)(R')$YCO complex in the reactions (from top) $Y+H_2CO$, $Y+CD_3CDO$, and $Y+(CH_3)_2CO$. Top two structures taken from Ref. 20. Bottom structure determined by analogy. Bond lengths are given in angstroms.

limit. The large rate constant for dissociation results from a relatively large total energy, shallow complex well, and loose transition state for CO elimination. The latter assumption is reasonable because the C–O bond length in the dissociating $(R)(R')$YCO intermediate is nearly the same as that of free CO [$r_{CO}=1.156$ Å for (H)(H)YCO (Ref. 20) and $r_{CO}=1.1283$ Å for CO (Ref. 24)]. The similarity in bond lengths also suggests that the CO product should not be vibrationally excited.

It is now becoming clear that reactions in which dissociation is faster than intramolecular vibrational redistribution (IVR) may be more common than previously thought. For example, in the S_N2 reaction $OH^-+CH_3F\rightarrow CH_3OH+F^-$, *ab initio* direct-dynamics trajectory calculations indicated that 90% of trajectories correspond to dissociation to products before complete IVR can occur.[27] Another example is methyl loss from the acetone radical cation generated by 1,3 H migration from the enol isomer. Direct-dynamics trajectory calculations showed preferential loss of the methyl formed upon hydrogen transfer despite the presence of an intermediate prior to dissociation lying 20 kcal/mol below the product asymptote.[28] In reactions involving Y atoms, a ''heavy atom'' effect may also be operable. Such an effect was observed by Scoles and coworkers in spectra of the fundamental and first overtone acetylenic C–H stretch of $(CH_3)_3CC{\equiv}CH$, $(CH_3)_3SiC{\equiv}CH$, and

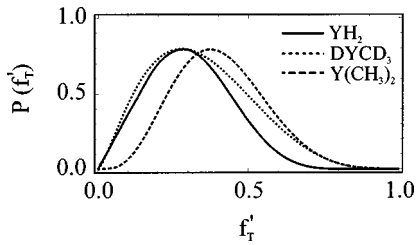

FIG. 8. Distributions of the product translational energy as a function of the fraction of available energy for the three reactions under study [i.e., the $P(E)$ scaled by the total available energy, E_T, for each reaction].

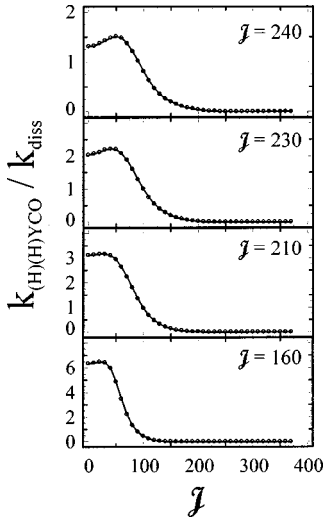

FIG. 9. Ratio of the RRKM rate constants for rearrangement of the pi-complex to the final dissociating complex (H)(H)YCO [$k_{(H)(H)YCO}$] to that for dissociation of the pi-complex back to reactants (k_{diss}) as a function of total angular momentum, $\mathscr{J}$. Collision energies are (from top), $\langle E_{coll}\rangle$ = 32.0 kcal/mol, 27.0 kcal/mol, 20.9 kcal/mol, and 5.0 kcal/mol. Inset values indicate when the ratio goes to zero.

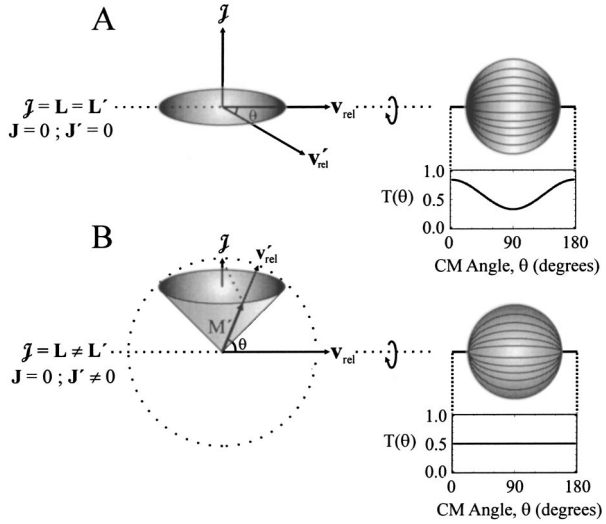

FIG. 10. Illustration of two extreme cases of total angular momentum partitioning as predicted by statistical complex theory, and the resulting center-of-mass angular distributions. (A) No rotational excitation of the products ($\mathbf{J}'=0$). (B) Products are rotationally excited ($\mathbf{J}'\neq 0$). See text for details.

$(CH_3)_3SnC{\equiv}CH$.[29,30] From the homogeneous linewidths, lifetimes of the initial vibrational excitation were observed to increase significantly with the mass of the central atom. This suggested that IVR from the initial C–H excitation into the terminal methyl groups (which accounted for most of the state density) was at least in part being slowed by the presence of heavier central atoms.[29,30] In a recent study of the reaction of $Co^+(^3F_4)$ with propane,[31] the large translational energy release for H_2 elimination was rationalized in terms of inefficient energy redistribution after passage over a multicentered transition state $(H_2)Co(C_3H_6)^+$ leading to products. Because potential energy coupling directly to the propene side of this transition state was weak, IVR through the heavy cobalt atom was slow relative to dissociation.[31] Similarly, in the $Y+RR'CO$ reactions, once R' migrates to the yttrium atom it is not directly coupled to CO (Fig. 6), so redistribution of energy from $Y-R'$ bond formation must occur through the heavy Y atom.

We conclude that the large translational energy release for CO elimination results from two factors: a large potential energy barrier for migration of the R' moiety to yttrium, and inability of excess energy to be completely randomized before dissociation to $RYR'+CO$ products.

2. Center-of-mass angular distributions

To explain the differences in the shape of the CM angular distributions for these CO elimination reactions we employ statistical complex theory, first applied by Herschbach[32] and later updated by Grice.[33] Approach of reactants with impact parameter **b** leads to formation of a complex, with total angular momentum $\mathscr{J}$ equal to the sum of the initial orbital angular momentum **L** and the initial rotational angular momentum **J**. Since reactant rotation is cooled in the supersonic expansion, for all practical purposes $\mathbf{J}\approx 0$.[34] The total angular momentum vector $\mathscr{J}$ is then approximately equal to **L**, lying perpendicular to the plane of complex rotation. When the complex decays, $\mathscr{J}$ is partitioned into product orbital angular momentum $\mathbf{L}'$ and rotational angular momentum $\mathbf{J}'$. Two cases will be discussed. The first case is where products receive relatively little rotational excitation ($\mathbf{J}'\approx 0$). In this case, $\mathbf{L}'\approx\mathbf{L}$, and products are constrained to the plane of initial approach [Fig. 10(a)] so $\mathbf{v}'_{\mathbf{rel}}$ is constrained to lie in the same plane as the initial relative velocity vector $\mathbf{v}_{\mathbf{rel}}$. Taking into account the cylindrical symmetry about $\mathbf{v}_{\mathbf{rel}}$, this yields a CM angular distribution that is forward–backward peaking (θ=0° and θ=180°), with a limiting case of $T(\theta)=1/\sin\theta$ when $\mathbf{L}=\mathbf{L}'$.[32] The second possibility occurs when the products are rotationally excited, or when $\mathbf{J}'$ is an appreciable fraction of $\mathscr{J}$ [Fig. 10(b)]. In this case, $\mathbf{L}'$ is not equal to **L**, so products can scatter out of the plane containing $\mathbf{v}_{\mathbf{rel}}$, yielding an isotropic CM angular distribution.[32]

The shape of $T(\theta)$ is related to a parameter X, given by[32]

$$X=\frac{|\mathbf{L}_{\mathbf{max}}|}{\langle\mathbf{M}'_{\mathbf{rms}}\rangle}, \tag{1}$$

where $\mathbf{L}_{\mathbf{max}}$ is the maximum orbital angular momentum of the complex, and $\langle\mathbf{M}'_{\mathbf{rms}}\rangle$ is the projection of the total angular momentum $\mathscr{J}$ onto the recoiling velocity vector $\mathbf{v}'_{\mathbf{rel}}$ [depicted as $\mathbf{M}'$ in Fig. 10(b)]. A large value of X indicates that $\langle\mathbf{M}'_{\mathbf{rms}}\rangle$ is small, or that $\mathbf{v}'_{\mathbf{rel}}$ is nearly in the same plane as $\mathbf{v}_{\mathbf{rel}}$, corresponding to the first case described above with a forward–backward peaking $T(\theta)$. By contrast, a small value of X means $T(\theta)$ is nearly isotropic. Following Grice,[35] we make the assumption that the orbital angular momentum is equal to its maximum value, i.e., $\mathbf{L}=\mathbf{L}_{\mathbf{max}}$ to get

$$\langle\mathbf{M}'_{\mathbf{rms}}\rangle=\left|\frac{\mathbf{L}^2_{\mathbf{max}}}{2}\left(\frac{I_{\parallel}}{I_{\perp}-I_{\parallel}}\right)\right|^{1/2}, \tag{2}$$

where $I_{\parallel}$ and $I_{\perp}$ are the moments of inertia of the complex parallel and perpendicular to its symmetry axis. Substituting Eq. (2) into Eq. (1) gives

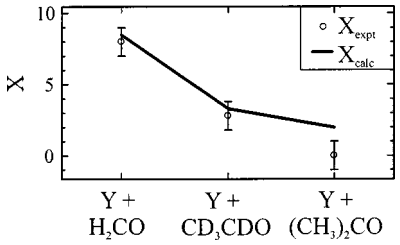

FIG. 11. The value of X plotted as a function of reaction. Open points are experimentally determined values; solid line connects values calculated using Eq. (3) and moments of inertia shown in Fig. 7.

$$X=\sqrt{2}\left(\frac{I_{\perp}-I_{\parallel}}{I_{\parallel}}\right)^{1/2}. \tag{3}$$

Equation (3) is a simple expression relating the shape of the CM angular distributions to the geometry of the dissociating complex through its moments of inertia.

The experimentally determined values of X for CO elimination from formaldehyde, acetaldehyde, and acetone are listed in Table II. The value of X is large for formaldehyde, and decreases to zero for acetone. Figure 11 shows a plot of the experimentally determined values of X along with those calculated using the structures and moments of inertia shown in Fig. 7 along with Eq. (3). We have assumed that the moments of inertia perpendicular to the C–O bond axis are the same at the transition state as for the complex. The calculated values show qualitative agreement with experimentally determined values.

The theory does overestimate the value of X for acetone, however. To understand why, one must note that a primary assumption in the statistical complex model is that the dissociating complex can be well approximated by a symmetric top, either as a prolate rotor ($I_{\perp}>I_{\parallel}$) (Refs. 32 and 33) or an oblate rotor ($I_{\perp}<I_{\parallel}$).[32,36] Our derivation of X assumes a prolate geometry of the dissociating complex. *Ab initio* structures[20] in Fig. 7 show the dissociating complex (H)(H)YCO to be a very good approximation to a prolate rotor, with $I_{\perp}/I_{\parallel}\approx 37$. In the case of (D)($CD_3$)YCO, $I_{\perp}/I_{\parallel}\approx 6$, while for ($CH_3$)($CH_3$)YCO $I_{\perp}/I_{\parallel}\approx 4$. Thus, the dissociating complex geometries go from being very prolate for formaldehyde to being much less so for acetone. This also helps explain the shape of the CM angular distributions for these reactions, in that as the dissociating complex becomes less prolate, the $T(\theta)$ becomes less forward–backward peaking, and moves toward the shape of angular distributions for oblate rotors, which are predicted by statistical complex theory to be peaking at $\theta=90°$.[32,36] Such ''sideways'' peaking $T(\theta)$s have been observed experimentally, for example in the reaction of $F+C_2H_4$.[37–39] It is therefore apparent that the accuracy of predictions made by statistical complex theory is dependent upon the structure of the dissociating complex and the quality of its approximation as a prolate rotor.

V. CONCLUSION

We have studied the reactions of ground-state yttrium atoms with formaldehyde, acetaldehyde, and acetone. Four product channels are observed at high collision energies for all three reactions, corresponding to elimination of H, H_2, CO, and nonreactive scattering. Elimination of CO from RR'CO proceeds via initial formation of a pi-complex with the carbonyl, followed by insertion into either the R–C or R'–C bond. Migration of R and R' to the metal center generates the final intermediate, $(R)(R')$Y(CO), which then decays to $RYR'+$CO. Product translational energy distributions for all three reactions show that a large amount of the available energy is deposited into product translation. This is attributed to a large potential energy barrier for formation of the $(R)(R')$YCO complex followed by fast dissociation to products without complete energy redistribution in the complex. Product CM angular distributions range from being very sharply forward–backward peaking in the case of formaldehyde to being isotropic in the case of acetone, as expected from changes in the moments of inertia of the decaying complexes.

ACKNOWLEDGMENTS

This work was supported by the ACS Petroleum Research Fund and by the National Science Foundation. Jonathan Schroden thanks the Department of Education and the Cornell Graduate School for a Fellowship. Special thanks to Ryan Hinrichs for many stimulating and enlightening conversations, to Craig Bayse for personal communications of *ab initio* data, and to Hans Stauffer for use of figures.

[1] K. J. Cavell, Coord. Chem. Rev. **155**, 209 (1996).
[2] E. Drent and P. H. M. Budzelaar, Chem. Rev. **96**, 663 (1996).
[3] R. C. Burnier, G. D. Byrd, and B. S. Freiser, Anal. Chem. **52**, 1641 (1980).
[4] R. C. Burnier, G. D. Byrd, and B. S. Freiser, J. Am. Chem. Soc. **103**, 4360 (1981).
[5] L. F. Halle, W. E. Crowe, P. B. Armentrout, and J. L. Beauchamp, Organometallics **3**, 1694 (1984).
[6] C. J. Carpenter, P. A. M. van Koppen, and M. T. Bowers, J. Am. Chem. Soc. **117**, 10976 (1995).
[7] S. S. Yi, E. L. Reichart, and J. C. Weishaar, Int. J. Mass. Spectrom. **185/186/187**, 837 (1999).
[8] H. U. Stauffer, R. Z. Hinrichs, J. J. Schroden, and H. F. Davis, J. Chem. Phys. **111**, 10758 (1999).
[9] H. U. Stauffer, R. Z. Hinrichs, P. A. Willis, and H. F. Davis, J. Chem. Phys. **111**, 4101 (1999).
[10] P. A. Willis, H. U. Stauffer, R. Z. Hinrichs, and H. F. Davis, J. Phys. Chem. A **103**, 3706 (1999).
[11] H. U. Stauffer, R. Z. Hinrichs, J. J. Schroden, and H. F. Davis, J. Phys. Chem. A **104**, 1107 (2000).
[12] R. Z. Hinrichs, J. J. Schroden, and H. F. Davis (unpublished).
[13] J. J. Carroll, K. L. Haug, J. C. Weishaar, M. R. A. Blomberg, P. E. M. Siegbahn, and M. Svensson, J. Phys. Chem. **99**, 13955 (1995).
[14] P. A. Willis, H. U. Stauffer, R. Z. Hinrichs, and H. F. Davis, Rev. Sci. Instrum. **70**, 2606 (1999).
[15] D. E. Powers, S. G. Hansen, M. E. Geusic, A. C. Puiu, J. B. Hopkins, T. G. Dietz, M. A. Duncan, P. R. R. Langridge-Smith, and R. E. Smalley, J. Phys. Chem. **86**, 2556 (1982).
[16] D. Proch and T. Trickl, Rev. Sci. Instrum. **60**, 713 (1989).
[17] Acetaldehyde-d_4 was used to avoid complications from yttrium oxide (YO, mass 105), present as a minor contaminant in the metal beam. This resulted in the CO elimination product being $DYCD_3$ (detected as mass 109) instead of $HYCH_3$ (mass 105).
[18] P. E. Siegbahn, Theor. Chim. Acta **87**, 441 (1994).
[19] J. Berkowitz, G. B. Ellison, and D. Gutman, J. Phys. Chem. **98**, 2744 (1994).
[20] (a) C. A. Bayse, J. Phys. Chem. A **106**, 4226 (2002); (b) personal communication.
[21] No *ab initio* calculations have been done on the Y+ acetone system, and

for comparison of the CM distribution (see Sec. III B) it was important to have consistent values of the reaction exothermicity.
[22] J. J. Low and W. A. Goddard III, J. Am. Chem. Soc. **106**, 8321 (1984).
[23] L. Zhu and W. L. Hase, Program 644, Quantum Chemistry Program Exchange, Indiana University.
[24] *CRC Handbook of Chemistry and Physics*, 75th ed., edited by D. R. Lide (CRC, Boca Raton, FL, 1995).
[25] J. J. Carroll, Ph.D. thesis, University of Wisconsin-Madison, 1995.
[26] P. A. M. van Koppen, D. B. Jacobson, A. Illies, M. T. Bowers, M. Hanratty, and J. L. Beauchamp, J. Am. Chem. Soc. **111**, 1991 (1989).
[27] L. Sun, K. Song, and W. L. Hase, Science **296**, 875 (2002).
[28] J. A. Nummela and B. K. Carpenter, J. Am. Chem. Soc. **124**, 8512 (2002).
[29] K. K. Lehman, B. H. Pate, and G. Scoles, J. Chem. Phys. **93**, 2152 (1990).
[30] E. R. Th. Kerstel, K. K. Lehman, T. F. Mentel, B. H. Pate, and G. Scoles, J. Phys. Chem. **95**, 8282 (1991).
[31] E. L. Reichert and J. C. Weisshaar, J. Phys. Chem. A **106**, 5563 (2002).
[32] (a) W. B. Miller, S. A. Safron, and D. R. Herschbach, Discuss. Faraday Soc. **44**, 108 (1967); (b) J. Chem. Phys. **56**, 3581 (1972).
[33] R. D. Jarvis and R. Grice, Mol. Phys. **65**, 1205 (1988).
[34] G. Scoles, *Atomic and Molecular Beam Methods* (Oxford University Press, New York, 1988), Vol. I., Chap. 1.
[35] R. D. Jarvis, J. J. Harkin, D. J. Smith, and R. Grice, Chem. Phys. Lett. **167**, 90 (1990).
[36] R. D. Jarvis and R. Grice, Mol. Phys. **66**, 675 (1989).
[37] J. M. Parson and Y. T. Lee, J. Chem. Phys. **56**, 4685 (1972).
[38] J. M. Parson, K. Shobatake, Y. T. Lee, and S. A. Rice, Faraday Discuss. **55**, 344 (1973).
[39] J. M. Farrar and Y. T. Lee, J. Chem. Phys. **65**, 1414 (1976).